Sediment characterization in 'De IJzermonding' using an empirical orthogonal function: application to CASI

Adam Stefanie[a], Suhyb Salama[a] and Jaak Monbaliu[a]

[a] Katholieke Universiteit Leuven, Departement Bouwkunde, Laboratorium voor Hydraulica, Kasteelpark Arenberg 40, 3001-Heverlee, Belgium
email: stefanie.adam@bwk.kuleuven.ac.be

ABSTRACT

The erodability of mudflats is strongly determined by bio-physical characteristics of sediments, such as silt, sand, benthic microalgae and water content. Mudflats are often large and inaccessible areas, leading to dangerous and time-consuming in situ measurement campaigns. Furthermore the collected point samples are unrepresentative for the spatial variability of these coastal systems. Airborne hyperspectral remote sensing is identified to be effective for the collection of a synoptic overview of bio-physical characteristics of sediments in mudflats.

In this paper an automated method for hyperspectral image classification is proposed. The method is based on a linear transformation of each spectrum in the hyperspectral cube. Different sediment types and land covers were classified using two dimensions of the transformed data space.

The methodology is applied to hyperspectral images of the IJzermonding mudflat, acquired by the Compact Airborne Spectrographic Imager (CASI-2). Comparable classification results are obtained using a standard classification method employed in hyperspectral image processing. The superiority of the proposed method lies in its robustness (no interference from the operator), computational requirements, repeatability, interpretability and objectiveness. The proposed method uses the underlying statistical information of the dataset while the standard method is mainly based on expert knowledge.

Keywords: mudflats, bio-physical characteristics, hyperspectral image classification, linear transformation.

1 INTRODUCTION

Coastal regions are very important from an ecological, coastal defence and economical (tourism, recreation, housing, employment, ...) point of view. These coastal areas and especially intertidal zones are at risk due to increasing pressure from human development and from climate change. Rising sea level and increasing frequency and intensity of storms might lead to an acceleration of mudflat erosion causing a threat for the hinterland and its economical values.

The process of sediment entrainment, transport and deposition is dependent upon the biological and physical characteristics of the sediment: cohesive sediments show a different erosion behaviour than non-cohesive sediments; cohesive sediments with a biofilm of microphytobenthic algae are less susceptible for erosion, but on the other hand, bioturbation by macrofaunal species will increase the erosion rate [1], [2], [3], [4], [5].

Bio-physical characteristics of intertidal zones are usually estimated or derived from field measurements by the application of interpolation techniques on point measurements. Field measurements are however spatially unrepresentative, especially for dynamic and heterogeneous intertidal mudflats. Furthermore field observations are seriously restricted by the limited accessibility and the short exposure time between tides. Remote sensing offers a means for the collection of area covering data. In particular, hyperspectral airborne remotely sensed images are promising for the study of intertidal zones because of the superior spectral and spatial resolution, and operational flexibility.

Researchers have tried to use remotely sensed images to characterize intertidal sediments. A supervised and unsupervised classification method of sediment and vegetation types of the Humber estuary gave good qualitative results. An accuracy assessment could not be performed due to poor field data of the study sites [6]. However other researchers could develop an empirical model for the quantitative estimation of sand and mud [7]. A spectral linear unmixing procedure using collected endmembers (spectra of pure materials) was applied on hyperspectral airborne imagery and an empirical model calibrated and validated using many field data. The accuracy and

prediction potential of the model were expressed as a correlation coefficient. The clay distribution could be mapped based on the mud abundance image with a correlation coefficient of 0.79. For the sand distribution the correlation was lower ($r^2 = 0.60$). This model however can only be used on that particular intertidal flat and for that image.

The main objective of this research is the extraction and interpretation of information from hyperspectral images. In order to achieve this objective two classification methods will be applied to hyperspectral images, evaluated and compared. The first classification procedure is based on a empirical orthogonal functions and will be presented here. As a reference, a standard classification procedure will also be applied.

2 STUDY AREA

The IJzer is a relatively small stream in the western part of Belgium with a short intertidal zone at the North Sea. Although human influence is considerable, the estuary of the IJzer has high ecological values. The dunes extend far in the hinterland and a small part of the right shore of the IJzer has never been artificially protected by constructions, assuring the presence of an intertidal flat with continuous transitions between beach and marsh, and marsh and dunes.

The nature reserve 'De IJzermonding' consists of the marshes and dunes that are protected since 1961, the former base of the army, the beach and surrounding areas, which makes a total of 103 ha. A nature restoration project was developed AMINAL [8]. During the monitoring phase between 2000 and 2004, high stability was noticed in the southern parts of the nature reserve where no significant changes occurred. The areas that have been changed considerably (near the outlet of the river) have been eroding and seem to evolve towards a new equilibrium state.

Some parts of the intertidal zone are covered by a biofilm of microphytobenthos, suggesting cohesive properties or the presence of a large amount of silt (> 10-15%), as observed in the field and indicated in previous research [2], [4], [9]. Note that all the sediments with grain size smaller than 63µm are called silt. The largest part of this intertidal zone is covered by a mixture of sand and silt. Some small areas that are only flooded during spring-tide are covered with marsh vegetation. There is a vegetated dike and a large sandy area above the high water line. The stabilized dunes are covered with dense vegetation (Fig. 1).

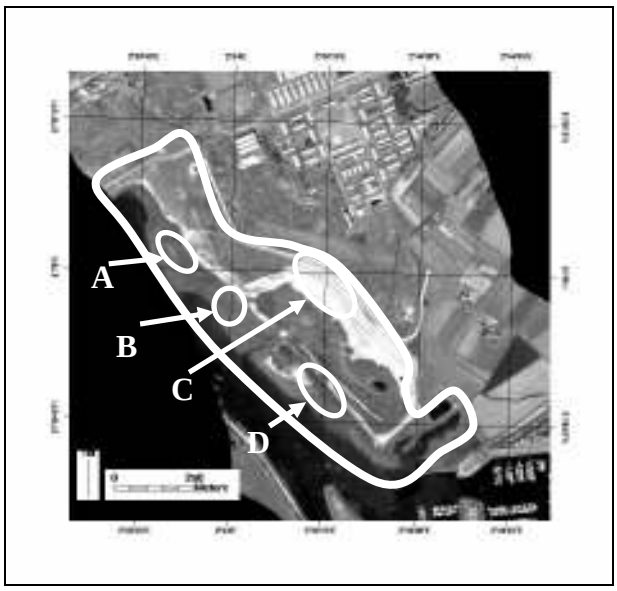

Figure 1. Overview of the study area with delineation of study area and indication of the most important land cover types. A: silt with biological influence, B: mixed sediment, C: sand, D: vegetated dike. Image acquired by CASI in 2003.

3 METHODS

3.1. Image Dataset

Hyperspectral images of the IJzermonding were acquired in August 2001 and June 2003 by the Compact Airborne Spectrographic Imager (CASI) (Table 1). The images will be called CASI 2001 and CASI 2003. CASI is a hyperspectral optical sensor measuring the reflectance in the visible (VIS) light and the near infra red (NIR) in many very narrow contiguous bands. The images have high spatial and spectral resolution and were radiometrically, and geometrically corrected by the operator of the instrument, while the atmospheric correction was performed by VITO (Vlaamse Instelling voor Technologisch Onderzoek).

Table 1. Characteristics of the available images

	CASI 2001	**CASI 2003**
Date	08-24-2001	06-16-2003
Moment of overflight	low tide, after a considerable time of air exposure	two hours after low tide
Spatial resolution	2m pixel size	2m pixel size
Spectral range	430-971nm	408-944nm
Spectral resolution	96 bands	48 bands
Radiometric resolution	8-bit	8-bit
Quality	Good	Good
Spatial coverage	IJzermonding not complete; only 1 flight line	IJzermonding complete, but partly flooded, due to late overpass of airplane

CASI 2001 had some bad bands due to stripes and bad visibility, namely in the blue region from 430nm to 475nm and in the NIR from 896nm to 971nm. These bands were removed and excluded from further analysis. For consistency the bands with these wavelengths were also removed in CASI 2003.

To minimize the spectral complexity of the image the regions of interest are isolated from all other spectral features. The area with the surrounding agricultural fields, the port, the beach and the buildings were not considered in the classification. The water is excluded by the application of a mask. This mask is built based on the principle that water absorbs almost all the NIR radiation.

3.2. Method Based on an Empirical Orthogonal Function

The vector character of most remote sensing image data renders it amenable to spectral transformations that generate new sets of bands. These components then represent an alternative description of the data, in which the new components of a pixel vector are related to its old brightness values in the original set of spectral bands via a linear operation. A commonly used linear transformation is the Principal Component transformation or Principal Component Analysis (PCA). This transformation finds a new set of orthogonal axes that have their origin at the data mean and that are rotated so that the data variance is maximised [10].

Principal component transformation is a powerful technique to decorrelate the bands so that the largest amount of information can be explained in a few bands. The classification of hyperspectral images can then be based on these few bands.

For the intertidal zone, the number of principal components (PCs) did not exceed two for both images to explain more than 99.2% of the data variation. The most important classes present in an intertidal zone are vegetation (on the stabilized dunes), silt, sand and mixed sediment (mixture of sand and silt). These classes show distinct properties in the NIR reflectance and red absorption, which is caused by the presence/absence of green pigment. It is expected that the first two PCs explain the variability in the NIR and the red reflectance. The first PC will differentiate between classes with high NIR reflectance (i.e. vegetation and sand) and classes with low NIR reflectance (silt and mixed sediment). The second PC will distinguish classes with green pigment (vegetation and silt) and classes without green pigment (sand and mixed sediment). High correlations were found between PC1 and NIR reflectance and between PC2 and red reflectance. The combination of the two PCs will enable us to separate four classes (Fig. 2).

The spectrum of vegetation has high intensities at the NIR and an absorption feature in the red, therefore the cluster of vegetation pixels will be situated in the first quadrant of the new axes (i.e. principal components). Sand shows high reflectances at the NIR, however no absorption feature at the red. In consequence sand pixels are expected to be in the fourth quadrant. The spectrum of silt with algae shows relatively low NIR reflectance and an absorption feature in the red: these pixels will be situated in the second quadrant. The fourth class contains pixels

with mixed sediment (sand mixed with varying amounts of silt) without absorption features and low NIR reflectance, so that these pixels will be found in the third quadrant.

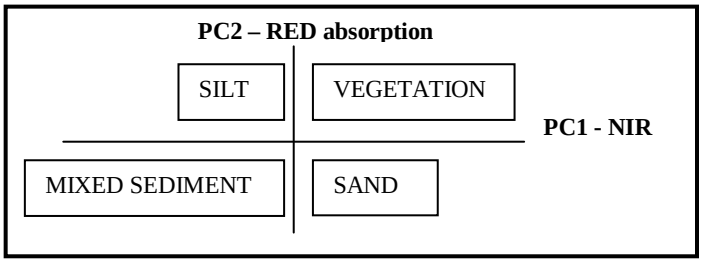

Figure 2. Physical interpretation of principal components

3.3. Standard Method

A common method used for the classification of hyperspectral images consists of several consecutive steps:

1) the minimum noise fraction transformation to reduce the dimensionality and to segregate noise [11].

2) the collection of the endmembers from the image by the determination of pure pixels and the visualization of these pure pixels in n-dimensions. When pixel data are plotted in a scatter plot that uses image bands as plot axes, the spectrally purest pixels always occur in the corners of the data cloud, while spectrally mixed pixels always occur on the inside of the data cloud. The endmembers correspond to pixels that contain one pure, particular material and are visually selected by identifying all the corners of the data cloud in n-dimensional space.

3) spectral angle mapper classification: the similarity of the spectrum of each pixel with the spectrum of the endmember is determined and expressed as a spectral angle between endmember and pixel spectrum. The pixel is assigned to the class for which it has the lowest spectral angle. A threshold angle for each class defines the minimum required similarity between pixel and endmember.

4 RESULTS AND DISCUSSION

4.1. Classification Using Principal Component Analysis

4.1.1 CASI 2001

Four regions of interest are delineated using the four quadrants of the scatterplot. A classification image (Fig. 3) is built on these four classes as explained in Sect. 3.2.

The spectral characteristics of the classes and field knowledge are used as basis for the identification and labelling of the clusters of pixels.

Based on field knowledge there is a large misclassification between silt with microphytobenthic algae and vegetation. Sparse vegetation was often misclassified as silt with microphytobenthic algae. Both classes have an absorption feature, but the NIR reflectance of vegetation is higher than the NIR reflectance of the silt pixels.

4.1.2 CASI 2003

The classification result of CASI 2003 shows the identification of a new class, namely another vegetation type. This type of vegetation is distinct from the first vegetation type because of the lower NIR reflectance. It is recognized in the image as sparse vegetation on wet sediment. The lower NIR reflectance might be due to the influence of bare sediment.

One of the classes actually consists of two distinct classes (silt + mixed sediment). These classes are separated based on the same principle: a principal component transformation followed by classification based on two PCs. This method is called ‘hierarchical’ principal component analysis (Fig. 4).

The identification of this class in CASI 2003 and not in CASI 2001 is caused by the large area of sparse vegetation that is covered in 2003 and excluded in 2001 (different spatial coverage). The influence of these pixels in the statistics is large and changes the contribution of each spectral band in the formation of the principal components.

This result indicates that some previous knowledge about the area is necessary. The number of the classes and the main spectral characteristics of each class should be known.

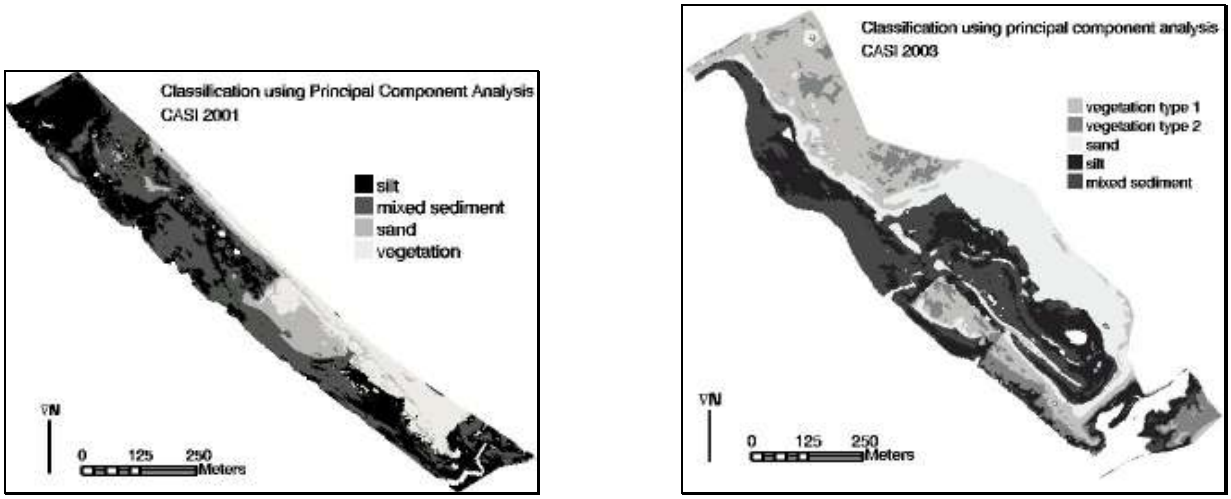

Figure 3. Classification results: CASI 2001 (left) and CASI 2003 (right)

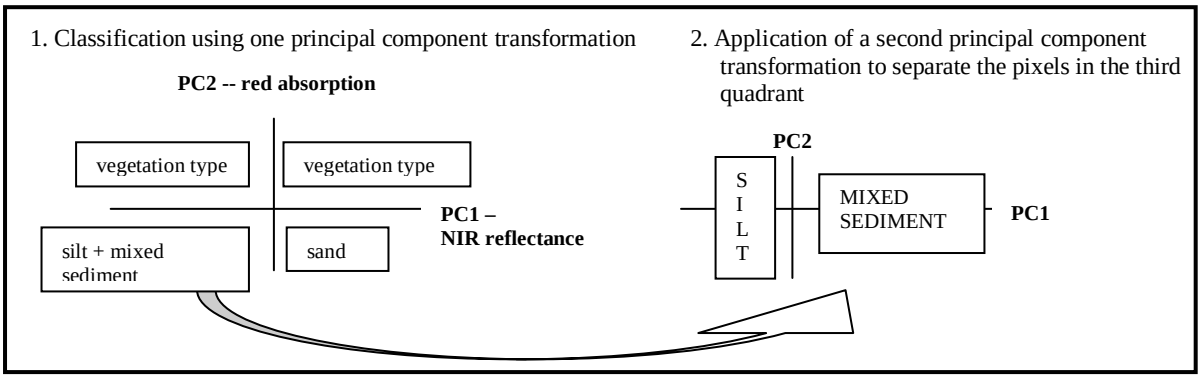

Figure 4. Classification using hierarchical principal component analysis – CASI 2003

4.2. Classification Using the Standard Method

The Minimum noise fraction transformation gathers all the information present in the original bands in the first few MNF bands. The spatial coherence of the first 12 MNF bands is large indicating that each band contains information about a spectral class in the image. Therefore it can be concluded that the inherent dimensionality of the data is 12, meaning that 12 different endmembers should be identified. It was however impossible to find 12 endmembers during the time-consuming and repetitive process of endmember collection using the visualization tool of the pure pixels in n-dimensions. Four endmembers (vegetation, silt, sand and mixed sediment) could be selected for the image of CASI 2001 and five endmembers (sparse vegetation included) for the image of CASI 2003. The SAM algorithm is applied to the image using these endmembers. The threshold angles can be chosen by the image interpreter based on terrain knowledge in order to improve the classification result.

4.3. Discussion

The overall similarity between the classification results of both methods (standard method and method based on PCA) was 61% for CASI 2003 and 44% for CASI 2001. The largest differences were found in the classes of sand, silt and mixed sediment. Since there is no ground reference available, it is not possible to decide which method is the most accurate. More research should be performed to estimate the accuracy of both methods.

However there are large differences in the classification procedures. The standard method is time-consuming (calculation of pure pixels and collection of endmembers) and very subjective (collection of endmembers, definition of threshold angle). It is mainly based on expert knowledge of the terrain and the image and on trial and

error. The results are not reproducible: the same image interpreter will not obtain the same results using the same image and method. The method cannot be automated, since the endmembers are derived from the image itself.

The classification method using PCA is objective and robust (no interference of image interpreter necessary) and it can be automated in a few steps. The procedure is fast and easy to perform, since it based on the statistics of the information content. The results are also physically interpretable.

Although the proposed method is easy to perform, some previous information about the number of classes and the spectral characteristics of each class is necessary. Therefore, the method is considered to be a semi-supervised classification method.

5 CONCLUSION

A classification procedure for intertidal mudflats based on an empirical orthogonal function, namely the principal component transformation was developed. The underlying mathematical basis of the method was studied so that the proposed classification procedure could be easily interpreted and understood.

The method was applied to two hyperspectral images. Inherent to the principal component transformation, the two first principal components explained most of the data variance, so that only these two bands were used for the classification of the images. The first PC caught the information in the NIR, the second PC the information in the VIS and more precisely the important red absorption feature. A hierarchical principal component classification was suggested if more than four classes were present in the image.

A standard method of hyperspectral image classification was applied to classify the images. Large differences were noticed between the results of both methods, but an accuracy assessment could not be performed due to lack of ground data. However the proposed method is superior with regard to user-friendliness, repeatability, ground truth requirements and physical interpretability.

ACKNOWLEDGMENTS

The images were acquired by the Natural Environment Research Council (NERC), UK. The radiometric, atmospheric and geometric correction was done by the Vlaamse Instelling voor Technologisch Onderzoek (VITO). This work was supported by the Belgian Science Policy (BELSPO) in the framework of the PRODEX Experiment Arrangement between ESA and the Katholieke Universiteit Leuven, project C90164 “The IJzer estuary”. We would like to thank the Institute for Land and Water Management (ILWM) of the KULeuven for the loan of equipment during field work.

REFERENCES

[1] AUSTEN, I., ANDERSEN, T.J., EDELVANG, K., 1999: The influence of benthic diatoms and invertebrates on the erodability of an intertidal mudflat, the Danish Wadden Sea. *Est. Coast. Shelf Sci. 49*, pp. 99-111.
[2] ANDERSEN, T.J., PEIRUP, M., 2002: Biological mediation of the settling velocity of bed material eroded from an intertidal mudflat, the Danish Wadden Sea. *Est. Coast. Shelf Sci. 54*, pp. 737-745.
[3] MITCHENER, H., TORFS, H., 1996: Erosion of mud/sand mixtures. *Coast. Eng. 29*, pp. 1-.25
[4] BRYANT, R., TYLER, A., GILVEAR, D., MCDONALD, P, TEADALE, I., BROWN, J., FERRIER, G., 1996: A preliminary investigation into the spectral characteristics of intertidal estuarine sediments. *Int. J. Remote Sens. 17*, pp. 405-412.
[5] CARRERE, V., 2003: Mapping microphytobenthos in the intertidal zone of Northern France using high spectral resolution field and airborne data. *3rd EARSeL Workshop on Imaging Spectroscopy, Herrsching, 13-16 May 2003*.
[6] THOMSON, A.G., EASTWOOD, J.A., YATES, M.G., FULLER, R.M., WADSWORTH, R.A., COX, R., 1998: Airborne remote sensing of intertidal biotopes: BIOTA I. *Mar. Pollution Bull. 37*, pp. 164-172.
[7] RAINEY, M.P., TYLER, A.N., GILVEAR, D.J., BRYANT, R.G., MCDONALD, P., 2003: Mapping intertidal estuarine grain size distributions through airborne remote sensing. *Remote Sens. Environ. 86*, pp. 480-490.
[8] HOFFMAN, M., HOYS, M., MONBALIU, J., SAS, M., 1996: Ecologisch streefbeeld en natuurherstelplan voor het integraal kustreservaat “de Ijzermonding” te Nieuwpoort-Lombardsijde met civieltechnische realisatiemogelijkheden. AMINAL.
[9] HUNTLEY, D., LEEKS, G., WALLING, D., 2001: Land-Ocean Interaction: Measuring and modelling fluxes from river basins to coastal seas. IWA Publishing.
[10] RICHARDS, J.A., 1986: Remote sensing digital image analysis: an introduction. Springer Berlin.

[11] GREEN, A.A., BERMAN, M., SWITZER, P., CRAIG, M.D., 1988: A transformation for ordering multispectral data in terms of image quality with implications for noise removal. *IEEE Trans. Geosci. Remote Sens. 26, no 1*, pp. 65-74.